

N O T I C E

THIS DOCUMENT HAS BEEN REPRODUCED FROM
MICROFICHE. ALTHOUGH IT IS RECOGNIZED THAT
CERTAIN PORTIONS ARE ILLEGIBLE, IT IS BEING RELEASED
IN THE INTEREST OF MAKING AVAILABLE AS MUCH
INFORMATION AS POSSIBLE

"Made available under NASA sponsorship
in the interest of early and wide dis-
semination of Earth Resources Survey
Program information without liability
for any use made thereof."

^{DSF}
E82-10327

CR-168906

INVESTIGATION NUMBER : M - 50

PRINCIPAL INVESTIGATOR : Jean-Louis LE MOUEL

PROGRESS REPORT of April 1, 1982

Models and maps of the main field.

by

Camille GIRE

Joël DUCRUIX

(E82-10327) MODELS AND MAPS OF THE MAIN
FIELD Progress Report (Paris VI Univ.)

13 p HC AC2/MF A01

CSCI 08R

N82-24600

Uncias

63/43 00327

RECEIVED

APR 30, 1982

SIS/902.6

7. PE II

M-050

MODELS AND MAPS OF THE MAIN FIELD

by

C. GIRE and J. DUCRUIX

OBJECTIVE :

The first objective of our investigation is to obtain some models of the main field. The difference between these models comes from the difference in the procedures of data selection and depends on the aim the model is intended for : regional studies necessitates locally higher density of data, for downward continuation the reduction of external variations must be as careful as possible. We present here refinements of our preliminary models MAGP1 and MAGP2 (see our progress reports entitled "Preliminary models of the core field") but these models are not yet definitive though they compare fairly well with those obtained by other teams (see for example Langel, 1981).

BACKGROUNDS :

Our models MAGP1 and MAGP2 were found to have drawbacks coming from insufficient reduction of the external variations and from the inhomogeneity in the distribution of the measurement points. New analysis has been performed to overcome these shortcomings. The quality of the new models had to be characterized by the average r.m.s. of the differences measurement-model as the facility of having profiles and maps rapidly drawn is not yet available to us.

This generation of models has the same general characteristics as the preceding one. The raw data have been averaged over 2.5s (this is approximately 18 km along the satellite track). To shorten the computations only one point out of sixty has been retained and the points above 60° of latitude have been discarded to lower the influence of the external perturbations. The component weighting has been kept to the same value : $p_x = 1.2$, $p_y = 0.6$ and $p_z = 0.8$.

We also keep the value $N = 11$ for the maximum order of the spherical harmonic development, this value being probably overestimated with respect to the precision obtained for the higher harmonic coefficients.

RECENT ACCOMPLISHMENTS :

We received the CHROFIN tapes from November 2nd 1979 to May 19th 1980. Four operations have to be made before having data ready for use in the spherical harmonic analysis. First translation from IBM binary code to CDC usable code, second averaging the measurements over a 2.5 second interval, third interpolating the satellite position and fourth determining the geomagnetic external activity index. This processing has been applied to the tapes containing the data from December 2nd 1979 to April 4th 1980 (CHROFIN tape number 8 to 22). In five files problems occur making the whole file unreadable (see arrows in Table 1). We have not found yet a solution to these problems.

spherical harmonic analysis :

We tested the influence of the polar regions on the quality of the models. We choosed a small subset of the data (from 12/02/79 to 12/06/79) containing 752 points having a magnetic activity index equal to 0 or 1 (for the meaning of this index see our progress report entitled "Separation of internal and external fields : a new technique of data screening"). Data points with a latitude larger than 60° were weighted with a weight P_0 varying between 0 and 0.1. The corresponding average r.m.s of the residues are displayed in Table 2. These results show no dramatic influence of the polar regions so we decided to discard these regions for our further analysis. However it has to be noted that the g_n^m and h_n^m coefficients are very stable for $n < 7$ and seems to be P_0 -dependant for $n > 7$.

We prepared three models using the data from 12/02/79 to 01/10/80. The first one called MGST01 used the same time interval of data as MAGP1 (from

12/01/79 to 12/21/79) with 2436 data points selected according to their index (0 or 1). The second one called MGST02 used no selection according to the external magnetic index and used 7247 measurements. The third one, MGST03, used 1996 data points with an index 0 or 1 belonging to the period 12/22/79 to 01/10/80. The average r.m.s of the residues of these models are displayed in Table 3. We decided to retain model MGST03 because the corresponding data points distribution is more uniform than for the MGST01 model. The g_n^{in} and h_n^{m} coefficient of the MGST03 model are shown in Table 4. The corresponding maps for the elements F, D, I and Z have been drawn (see figures 1 to 4).

anomaly maps :

Tentative anomaly maps have been computed but are not yet satisfactory. We used $5^\circ \times 5^\circ$ averaging which is too coarse and the external variation reduction needs to be refined. Further attempts are to be made (see next section).

secular variation :

The secular variation is smaller than 0.5nT/day all over the surface of the Earth. Then we decided to neglect this variation as a first approximation the resulting error being lower than 10 nT for our MGST03 model. We undertook a detailed study of the secular variation (Ducruix et al, 1980; Le Mouél et al, 1982) and we will apply our knowledge to the preparation of a precise spherical harmonic model of the secular variation (see next section).

FUTURE EMPHASIS :

Our next step is the obtaining of precise anomaly maps. The critical point for this is the reduction of the external variation which is starting now using manual screening. We are also developing a algorithm of automatic screening based on pattern recognition but this will probably take some time to be achieved.

The secular variation will be described and taken into account using our model and a new method which will be displayed in our final report. We begun the analysis of the motion at the core surface corresponding to the secular variation by downward continuation of the main field at the core mantle boundary (see for example Madden and Le Mouél, 1982).

REFERENCES :

- DUCRUIX, J., COURTILOT, V. and J.L. LE MOUEL, 1980, Geophys.J.R.Astr.Soc., 61, 73-94.
- LANGEL, R.A., 1981, E.O.S., 62, 269 (abstract)
- LE MOUEL, J.L., DUCRUIX, J. and C. HA DUYEN, 1982, Phys. Earth Planet.Int., in the press.
- MADDEN, T. and J.L. LE MOUEL, 1982, Phil.Trans.A , in the press.

TABLE 1

CHROFIN file number	Corresponding date	Number of processed days
8A	12/02-06	4
8B	06-10	4
9A	10-14	4
9B	14-18	4
10A	18-22	4
10B	12/22-26	4
11A	26-30	4
11B	30-01/03	4
12A	03-07	4
12B	07-11	4
13A	01/11-15	4
13B	15-19	4
14A	19-23	0.8 ←
14B	23-27	4
15A	27-31	4
15B	01/31-02/04	4
16A	04-08	4
16B	08-12	4
17A	12-16	0.8 ←
17B	16-20	4
18A	02/20-24	4
18B	24-28	4
19A	28-03/03	0.7 ←
19B	03-07	0.2 ←
20A	07-11	4
20B	03/11-15	0 ←
21A	15-19	4
21B	19-23	4
22A	23-27	4
22B	27-31	4

ORIGINAL PAGE IS
OF POOR QUALITY

TABLE 2

Po	av. RMSX	av. RMSY	av. RMSZ
0	23.5	24.4	17.7
0.001	23.6	24.6	17.8
0.01	24.2	24.9	19.2
0.05	24.9	25.1	19.9
0.1	25.3	25.2	19.9

TABLE 3

	av. RMSX	av. RMSY	av. RMSZ
MGST01	20.6	20.4	14.2
MGST02	27.1	30.0	18.4
MGST03	20.0	13.9	13.6

TABLE 4 : MGST03 coefficients

	g_n^m	h_n^m
1 0	-29961	
1 1	-1992	5591
2 0	-1998	
2 1	3040	-2109
2 2	1666	-178
3 0	1310	
3 1	-2178	-348
3 2	1247	287
3 3	838	-236
4 0	937	
4 1	781	219
4 2	401	-251
4 3	-419	45
4 4	206	-291
5 0	-186	
5 1	358	49
5 2	258	152
5 3	-72	-152
5 4	-160	-82
5 5	-51	90
6 0	50	
6 1	65	-14
6 2	41	95
6 3	-194	66
6 4	5	-43
6 5	13	-2
6 6	-108	13
7 0	99	
7 1	-58	-81
7 2	1	-29
7 3	20	-5
7 4	-13	16
7 5	0	18
7 6	12	-23
7 7	-1	-10
8 0	20	
8 1	6	6
8 2	1	-18
8 3	-11	3
8 4	-6	-22
8 5	4	9
8 6	2	16
8 7	7	-13
8 8	0	-15
9 0	25	
9 1	12	-20
9 2	0	14
9 3	-13	8
9 4	10	-5
9 5	-3	-6
9 6	-1	9
9 7	6	10
9 8	1	-6
9 9	-5	2

TABLE 4 (continued)

	ϵ_n^m	h_n^m
10 0	-1	
10 1	-5	0
10 2	3	1
10 3	-5	1
10 4	-3	6
10 5	5	-4
10 6	3	0
10 7	1	-1
10 8	2	4
10 9	3	0
10 10	0	-6
11 0	12	
11 1	0	2
11 2	-2	0
11 3	2	-2
11 4	0	-3
11 5	-1	1
11 6	0	0
11 7	2	-2
11 8	2	0
11 9	-1	-1
11 10	2	-1
11 11	4	1

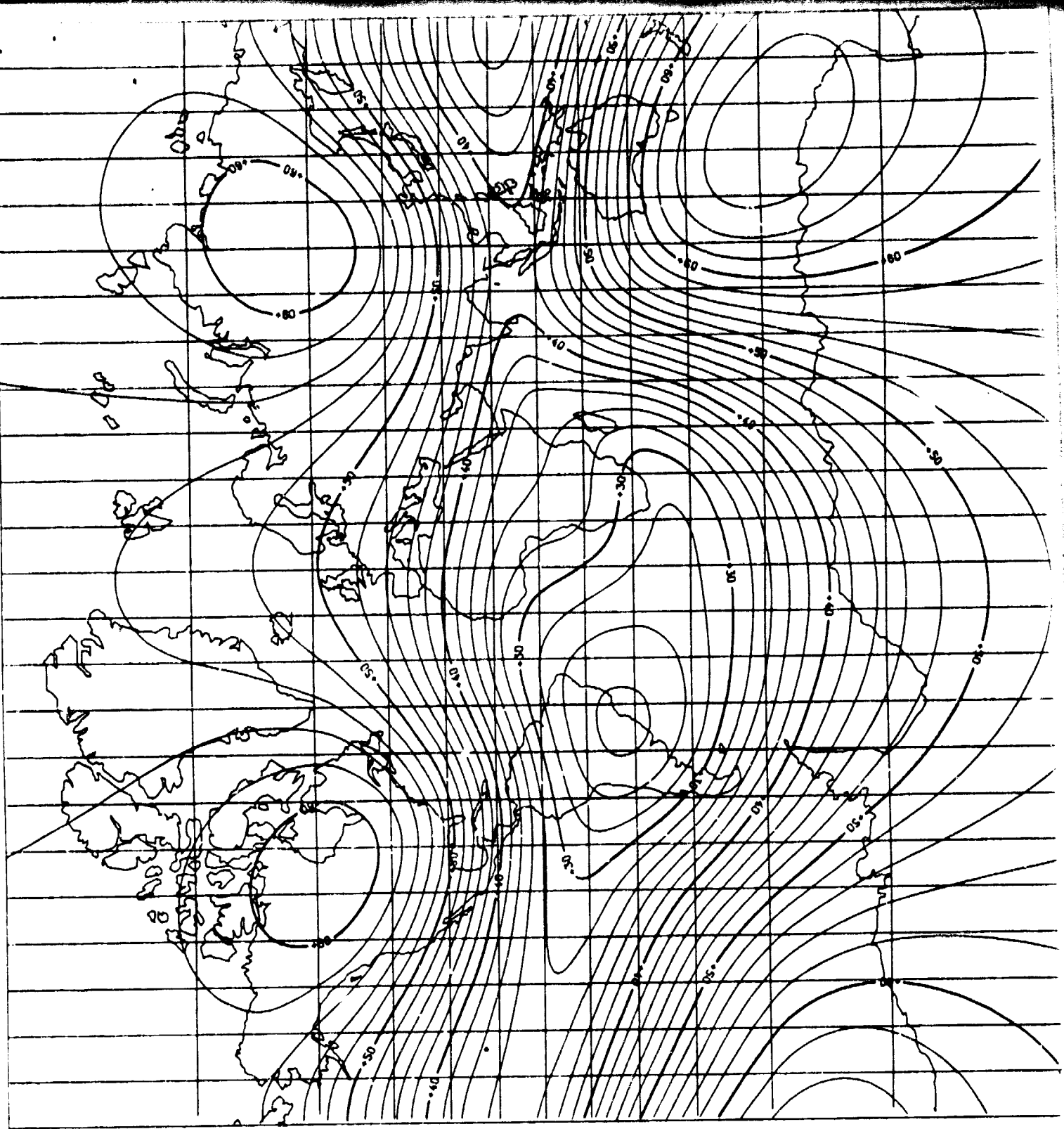


FIGURE 1

DISTRIBUTION OF F VALUES DISPLAYED
ON A MERCATOR CYLINDRICAL PROJECTION.
ISOVALUE LINES ARE 2000 FT APART.
VALUES ON THICK LINES ARE IN 10^3 FT.

ORIGINAL PAGE IS
OF POOR QUALITY.

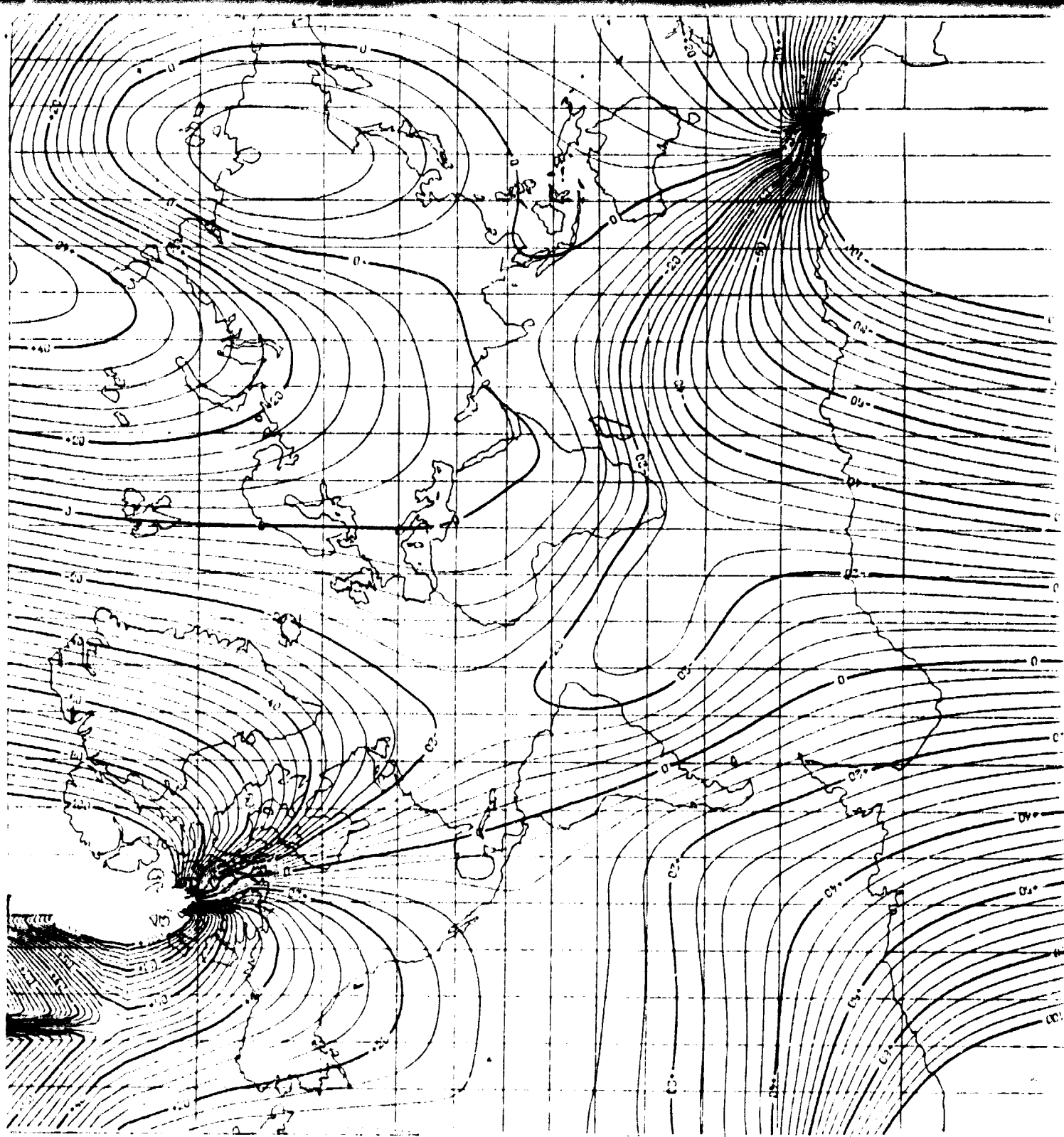


FIGURE 2

DISTRIBUTION OF D VALUES DISPLAYED
ON A MERCATOR CONFORMAL PROJECTION.
ISOVALUE LINES ARE 4° APART.

ORIGINAL PAGE IS
OF POOR QUALITY

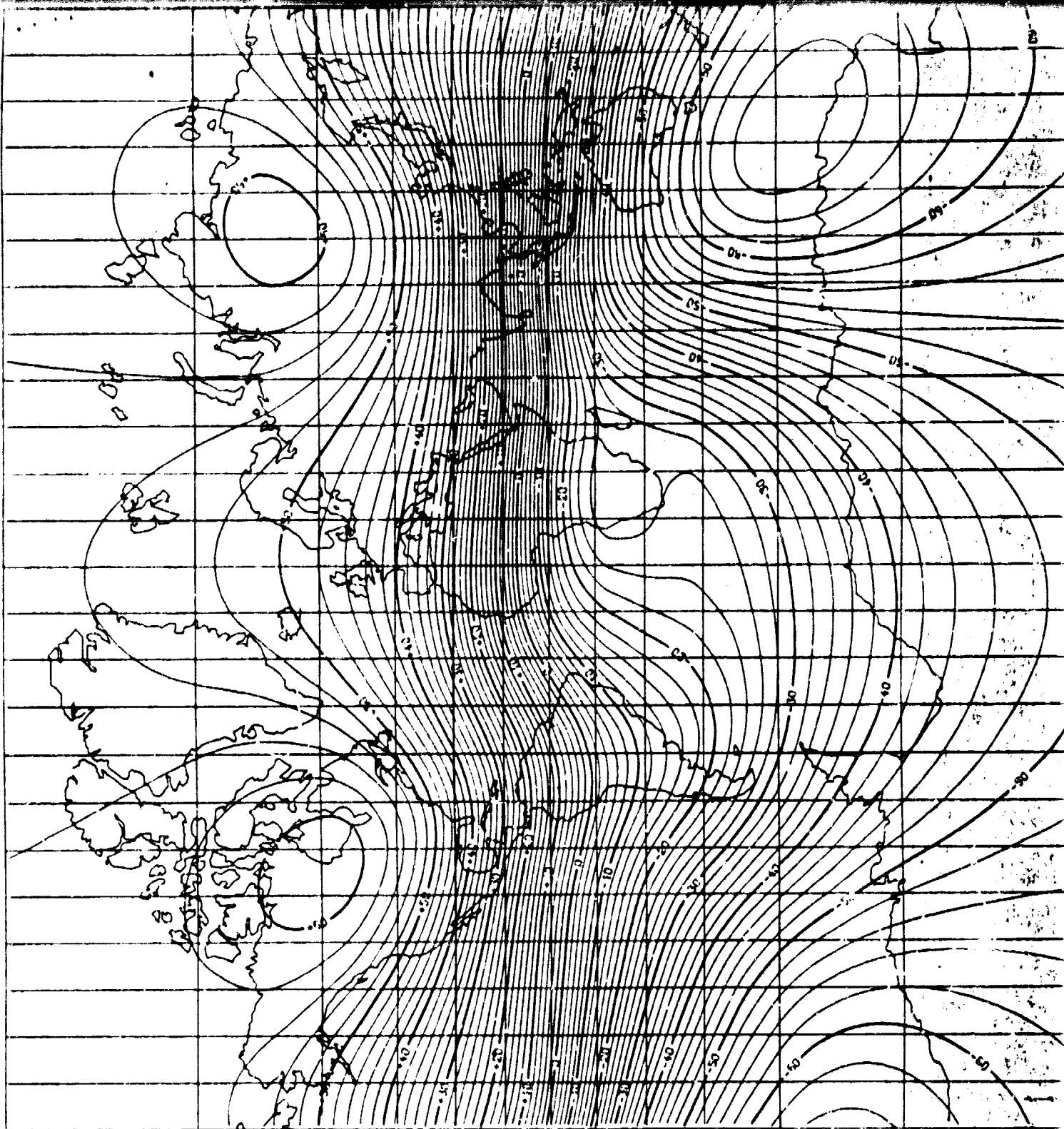


FIGURE 4

DISTRIBUTION OF Z VALUES DISPLAYED
ON A MERCATOR CONFORMAL PROJECTION.
ISOVALUE LINES ARE 2000 m APART.
VALUES ON THICK LINES ARE IN 10^3 m.

ORIGINAL PAGE IS
OF POOR QUALITY